

Taher Abedinzadeh^{1,*}, Mehdi Ehsan² and M.R. Jahed-Motlagh³

¹Department of Electrical Engineering, Science and Research Branch, Islamic Azad University, Tehran, Iran

²Department of Electrical Engineering, Sharif University of Technology, Tehran, Iran

³Department of Computer Engineering, Iran University of Science and Technology, Tehran, Iran

* (E-mail: taherabedinzade@yahoo.com)

ABSTRACT

This paper presents an improved method for calculation of rotor position and speed of a wound rotor induction machine. Rotor position is computed with using the measured stator and rotor voltages and currents without any information about the rotor flux. The algorithm is a very implicit procedure and there is no need for computing the stator flux. The method is robust to parameter variations in stator and rotor resistances. Starting on the fly, accurate computation and immunity against stator voltage fluctuations are the other advantages of this method. Simulation results demonstrate desired steady-state and dynamic performance of this sensorless rotor speed computation method for DFIG.

KEY WORDS-Doubly fed induction generator (DFIG), parameter sensitivity, sensorless rotor position computation, vector control.

INTRODUCTION

There are several applications, like wind turbines and hydroelectric pumping stations, where small changes on rotor speed cause considerable profits (Figure 1). Doubly fed induction generator (DFIG) is very attractive for variable-speed generation, especially for wind energy conversion systems (WECSs), where it is driven by the wind turbine. In this system, both stator and rotor circuits are connected to the mains. The applied rotor voltage through back-to-back power electronic based converter controls the real and reactive powers and generator's speed, when its stator terminals are connected to a power system and the stator voltage is held constant by the grid. There are so many advantages of using DFIG-based variable-speed wind turbines (Muller et al. 2002). First, the extracted mechanical power of wind turbine can be controlled to its maximum and converted by adjusting machine speed and electromagnetic torque. Second, only a fraction of the nominal electric power flows through the power converter, thus reducing its loss and cost. Yet, stator-side active and reactive powers can be independently controlled.

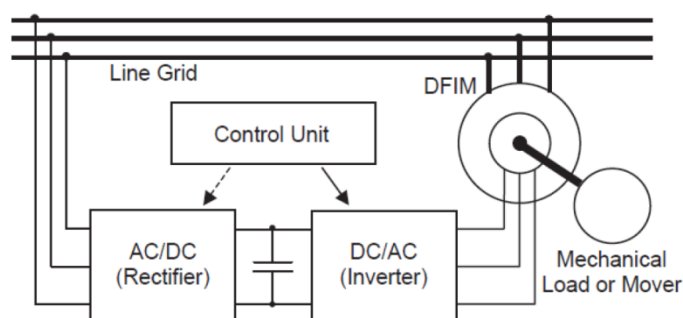


Figure 1: Block diagram of the DFIG system

There are several approaches for the control of the DFIG. The conventional control system of DFIGs is based on the stator-flux-oriented vector control (Ourici 2012, Tapia et al. 2006). Other methods like the stator voltage orientation, the direct power (Hu et al. 2010, Shehata and Salama 2013, Zhi and Xu 2007), or the direct torque control (Tremblay et al. 2011, Vas 1998, Zhang et al. 2011) are also studied and used industrially. In all the methods accomplished, the mechanical position of the rotor should be available that would be derived from a position encoder or from a sensorless algorithm as considered in this paper.

Because of easy installation, maintenance, high reliability and lower cost, the sensorless control methods have been preferred in a few past decades (Amuthan et al. 2013, Chena et al. 2012, Datta and Ranganathan 2001, Dezza et al. 2012, Iacchetti 2010, Iacchetti 2011, Karthikeyan et al. 2012, Krzeminski et al. 2001, Marques et al. 2011, Marques and Sousa 2011, Marques and Sousa 2012, Pena et al. 2008, Teja et al. 2012, Yang and Ajjarapu 2010). Major aspects should be considered in designing a position sensorless system for a DFIG. The algorithm should have stability and accuracy at any speed of the working range including near the synchronous speed. The rotor estimation position system should be able to start on the fly, which means, when the system starts working, the correct position and speed should be given after some period of time, without the knowledge of any initial condition (Datta and Ranganathan 2001, Marques and Sousa 2012).

Several position sensorless methods have been proposed in recent years. Mainly, the estimation algorithms can be categorized in two major groups: open loop and closed loop. The sensorless methods presented in (Datta and Ranganathan 2001, Krzeminski et al. 2001) are open loop and are based on the estimation of the rotor currents. Comparison between the estimated and measured rotor currents will result in the rotor position. In (Karthikeyan et al. 2012), a sensorless method that uses only the measured stator voltage and currents in stator and rotor windings was reported. The flux is not needed to be computed and is substituted with analytical equivalents in terms of measurable stator and rotor. Considering the grid or stator flux variation, the estimation of the stator flux is inaccurate, resulting in a poor performance.

Closed-loop model reference adaptive system (MRAS) technique or phase-locked loop methodologies have been proposed and studied in (Amuthan et al. 2013, Chena *et al.* 2012, Dezza et al. 2012, Iacchetti 2010, Marques et al. 2011, Marques and Sousa 2011, Marques and Sousa 2012, Teja et al. 2012). Commonly the adaptive models are based on static flux-current relations and either the current or the flux in the rotor or stator is considered as the tuning signal for driving the adaptation mechanism. Therefore, they are very sensitive to the machine inductance. Some of these observers are implemented on the rotor reference frame (Pena et al. 2008) and the others are implemented in the stator reference frame (Yang and Ajjarapu 2010). Estimation of angles of the stator flux vector and the actual rotor position and difference between these two angles is the key in stator flux orientation to implement the reference frame transformation. The controller of these MRAS observers is commonly a proportional-integral (PI) controller (Dezza *et al.* 2012, Iacchetti 2011, Yang and Ajjarapu 2010) or a hysteresis controller (Marques et al. 2011).

In (Marques and Sousa 2011), the slip angle is estimated by the phase comparison of measured value of the rotor current in the rotor reference frame with its estimated value in another reference frame based on air gap power vector. While a speed-adaptive reduced order observer is used in (Yang and Ajjarapu, 2010). The common disadvantage for MRAS observers is that they are

implemented in the stationary reference frame, where the electrical states are usually sinusoidal functions of time in steady state. Hence, it is difficult to design controller parameters, and the observer might become inaccurate or even unstable in digital implementation (Yang and Ajjarapu, 2010). This paper presents a new and simple approach for a sensorless algorithm to compute directly the rotor position in a straightforward manner without the estimation of the stator flux. This paper presents the method, its parameter sensitivity analysis and simulation. This unique computation algorithm has not been reported in the literature earlier. Conversely to others, the method does not use any intermediate estimated variable. It uses only the measured rotor and stator current and stator voltage to directly compute rotor angle. Accurate computation and immunity against stator voltage fluctuations are the other advantages of this method. Although it is an open-loop method, it does not involve the voltage integration, recursive or inverse trigonometric computations in real time. The method is robust to parameter variations in stator and rotor resistances. Simulation results demonstrate desired steady-state and dynamic performance of this sensorless rotor speed computation method for DFIG. Simulations are presented to validate the effectiveness of the schemes proposed in this paper. The rest of this paper is organized as follows. In Section II, the detailed explanation of the computation algorithm is introduced. Parameter sensitivity of the proposed method is presented in section III. Simulation results based on the MATLAB/Simulink environment are presented in Section IV. Section V presents the conclusion.

THE COMPUTATIONAL ALGORITHM

This paper presents a new procedure to compute the mechanical position of the rotor. The estimation of the rotor position can be performed using the mechanism shown in Figure 2. The stator current is, the rotor current i_r , and the stator voltage v_s , are used for the estimation of rotor position and speed. The spatial allocation of the rotor current vector in different frames of reference is shown in Figure 3.

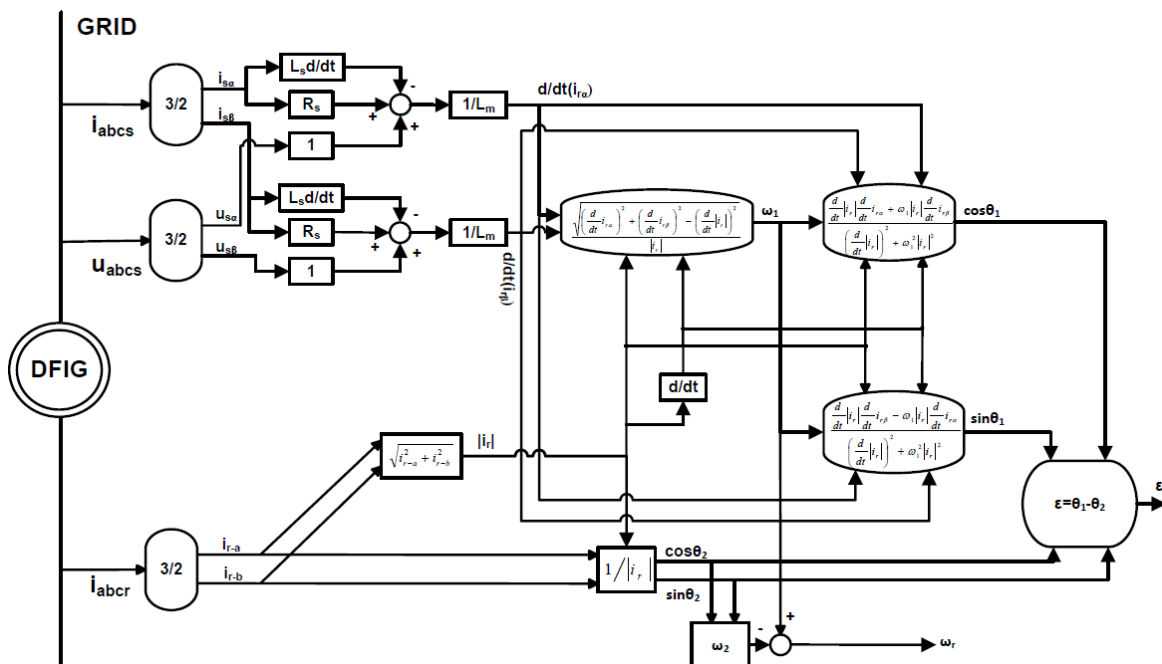


Figure 2: Rotor position and speed computation scheme

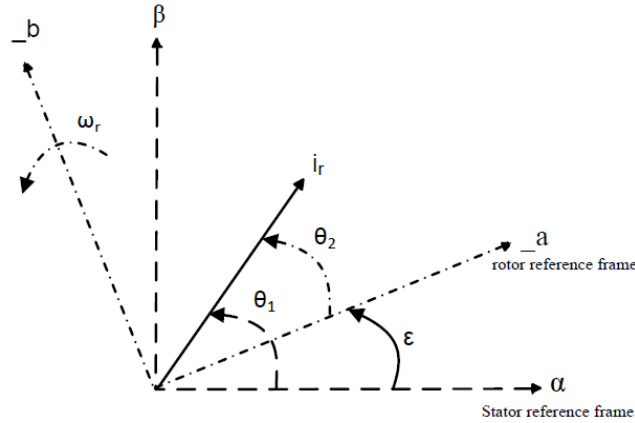


Figure 3: Spatial distribution of rotor current vector.

The rotor current i_r makes an angle θ_1 with respect to the α -axis of stator reference frame and an angle θ_2 with respect to the a -axis of rotor reference frame. Therefore, the required rotor position is obtained from difference between angles θ_1 and θ_2 . Hereafter, the steps of the algorithm is explained as follows.

Step 1: The angle in rotor reference frame (θ_2)

Because the rotor winding currents can be measured, with using the abc to $_{a_b}$ transformation, the $_{a_b}$ components of rotor current i_r in rotor reference frame can be computed. So, $\sin(\theta_2)$ and $\cos(\theta_2)$ can be calculated as:

$$\sin \theta_2 = \frac{i_{r_a}}{\sqrt{i_{r_a}^2 + i_{r_b}^2}}$$

$$\cos \theta_2 = \frac{i_{r_b}}{\sqrt{i_{r_a}^2 + i_{r_b}^2}} \quad (1)$$

And the magnitude of rotor current can be computed as:

$$|i_r| = \sqrt{i_{r_a}^2 + i_{r_b}^2} \quad (2)$$

Subsequently, the rotor current angular velocity in rotor reference frame can be expressed as (Datta and Ranganathan 2001, Karthikeyan et al. 2012):

$$\omega_2 = \cos(\theta_2) \frac{d}{dt} \sin(\theta_2) - \sin(\theta_2) \frac{d}{dt} \cos(\theta_2) \quad (3)$$

Step 2: The angle in stator reference frame (θ_1)

The angle of rotor current with respect to the α -axis of stator reference frame can be computed in an implicit manner without the need for stator flux estimation or the stator magnetizing current i_{ms} (or considering the time derivative of the stator flux magnitude negligible as proposed in (Karthikeyan et al. 2012)). The method is based on using measurable stator and rotor quantities to compute the angle θ_1 . The magnitude of measured rotor current and its time derivative used in this section are substituted from step 1.

Consider the following flux equations of the stator circuits on the stator reference frame:

$$\begin{aligned} \varphi_{s\alpha} &= L_s i_{s\alpha} + L_m i_{r\alpha} \\ \varphi_{s\beta} &= L_s i_{s\beta} + L_m i_{r\beta} \end{aligned} \quad (4)$$

From the above, the rotor currents in the stationary reference frame can be achieved as:

$$i_{r\alpha} = \frac{\varphi_{s\alpha} - L_s i_{s\alpha}}{L_m}$$

$$i_{r\beta} = \frac{\varphi_{s\beta} - L_s i_{s\beta}}{L_m} \quad (5)$$

The stator voltage in the stationary reference frame is given by the following:

$$v_{s\alpha} = R_s i_{s\alpha} + \frac{d}{dt} \varphi_{s\alpha}$$

$$v_{s\beta} = R_s i_{s\beta} + \frac{d}{dt} \varphi_{s\beta} \quad (6)$$

By derivation of (4) and also substituting (6) into them, it results:

$$\frac{d}{dt} i_{r\alpha} = \frac{\left(v_{s\alpha} - R_s i_{s\alpha} - L_s \frac{d}{dt} i_{s\alpha} \right)}{L_m}$$

$$\frac{d}{dt} i_{r\beta} = \frac{\left(v_{s\beta} - R_s i_{s\beta} - L_s \frac{d}{dt} i_{s\beta} \right)}{L_m} \quad (7)$$

A mathematical model of rotor current described by space vectors in a stationary frame can be expressed as follows:

$$i_{r\alpha} = |i_r| \cos \theta_1$$

$$i_{r\beta} = |i_r| \sin \theta_1 \quad (8)$$

By derivation of (8):

$$\sin \theta_1 = \frac{\frac{d}{dt} i_{r\alpha} - \cos \theta_1 \frac{d}{dt} |i_r|}{-\omega_1 |i_r|} \quad (9)$$

$$\cos \theta_1 = \frac{\frac{d}{dt} i_{r\beta} - \sin \theta_1 \frac{d}{dt} |i_r|}{\omega_1 |i_r|} \quad (10)$$

By dividing (8) to (9), it results:

$$\cos \theta_1 \frac{d}{dt} i_{r\alpha} + \sin \theta_1 \frac{d}{dt} i_{r\beta} = \frac{d}{dt} |i_r| \quad (11)$$

The equation of rotor current angular velocity in stator reference frame can be computed by using the squared (9) and (10) and substituting (11):

$$\omega_1 = \frac{\sqrt{\left(\frac{d}{dt} i_{r\alpha} \right)^2 + \left(\frac{d}{dt} i_{r\beta} \right)^2 - \left(\frac{d}{dt} |i_r| \right)^2}}{|i_r|} \quad (12)$$

Finally, with substituting (9) in (10) and vice versa, the required equations for computing the angle of rotor current with respect to the α -axis of stator reference frame can be obtained. All of these variables are related with the measured rotor currents. So the relationship between the angle θ_1 and other calculated amounts based on measured rotor current can be written as:

$$\cos\theta_1 = \frac{\frac{d}{dt}|i_r|\frac{d}{dt}i_{r\alpha} + \omega_1|i_r|\frac{d}{dt}i_{r\beta}}{\left(\frac{d}{dt}|i_r|\right)^2 + \omega_1^2|i_r|^2}$$

$$\sin\theta_1 = \frac{\frac{d}{dt}|i_r|\frac{d}{dt}i_{r\beta} - \omega_1|i_r|\frac{d}{dt}i_{r\alpha}}{\left(\frac{d}{dt}|i_r|\right)^2 + \omega_1^2|i_r|^2} \quad (13)$$

The probable noise originating from the differential terms can be eliminated by employing a first-order low-pass filter.

Step 3: Rotor position angle ($\theta_1 - \theta_2$)

The rotor position ($\varepsilon = \theta_1 - \theta_2$) can be obtained in terms of sine and cosine with knowing the unit vectors $\sin(\theta_2)$, $\cos(\theta_2)$, $\sin(\theta_1)$, and $\cos(\theta_1)$ from steps 1 and 2. The rotor position unit vectors $\sin(\varepsilon)$ and $\cos(\varepsilon)$ can be expressed as:

$$\cos(\varepsilon) = \cos(\theta_1)\cos(\theta_2) + \sin(\theta_1)\sin(\theta_2)$$

$$\sin(\varepsilon) = \sin(\theta_1)\cos(\theta_2) - \cos(\theta_1)\sin(\theta_2) \quad (14)$$

Eventually, the rotor speed can be computed as:

$$\omega_r = \omega_1 - \omega_2 \quad (15)$$

The notable advantage of this method is that there is no need to calculate or estimate the stator flux and the rotor angle is computed in a straightforward manner.

PARAMETER SENSIVITY

For the implementation of the proposed algorithm, the machine parameters R_s , L_s and L_m are required. From the tests on the machine, only their estimated values are available. In reality, parameter variations are unavoidable due to the temperature increase and magnetic saturation, so they can differ from the actual values. Therefore, a study considering machine parameter variations is necessary. The influences of each machine parameter variations on the speed and angle estimation are investigated by deriving the relationship between the speed and angle estimation error and the parameter mismatch.

As explained in the previous section, the measured rotor current in the rotor reference frame and the computed derivative of rotor current in the stator reference frame are used in the computational algorithm. The measured rotor current cannot be changed because of the any mismatch in the machine parameters, so only the computed derivative of rotor current (in stationary reference frame) can be affected and subsequently it will lead to an error in the computed rotor position.

First, the influence of stator resistance variation is studied. The change in computed rotor speed can be written as follows after some algebraic manipulations:

$$\Delta\omega_r = -\frac{\Delta R_s}{L_m\omega_1} \left(i_{s\alpha} \frac{d}{dt}i_{r\alpha} + i_{s\beta} \frac{d}{dt}i_{r\beta} \right) \quad (16)$$

$$\Delta(\cos\theta_1) = -\frac{i_{s\alpha} \frac{d}{dt}|i_r| + \omega_1|i_r|i_{s\beta}}{L_m \left(\left(\frac{d}{dt}|i_r| \right)^2 + \omega_1^2|i_r|^2 \right)} \Delta R_s \quad (17)$$

$$\Delta(\sin \theta_1) = -\frac{i_{s\beta} \frac{d}{dt} |i_r| - \omega_1 |i_r| i_{s\alpha}}{L_m \left(\left(\frac{d}{dt} |i_r| \right)^2 + \omega_1^2 |i_r|^2 \right)} \Delta R_s \quad (18)$$

In the above numerators, because the multipliers are much smaller than denominators, then $\Delta\omega_r$, $\Delta(\sin\theta_1)$ and $\Delta(\cos\theta_1)$ can be considered negligible.

Finally, the effects of mutual inductance variation are investigated. An analytical relationship between the rotor current angular velocity error and mutual inductance error has been extracted as follow:

$$\Delta\omega_r = -\frac{\Delta L_m}{L_m \omega_1 |i_r|^2} \left(\left(\frac{d}{dt} i_{r\alpha} \right)^2 + \left(\frac{d}{dt} i_{r\beta} \right)^2 + \frac{d}{dt} i_{s\alpha} \frac{d}{dt} i_{r\alpha} + \frac{d}{dt} i_{s\beta} \frac{d}{dt} i_{r\beta} \right) \quad (19)$$

Based on (19), the rotor speed error is proportional to rotor current angular velocity inverse value, as shown in Figure. 4. It means the error increases when the rotor current angular velocity in stator reference frame decreases. In this case, the error is obtained using MATLAB/Simulink (considering $\Delta L_m = 50\%$).

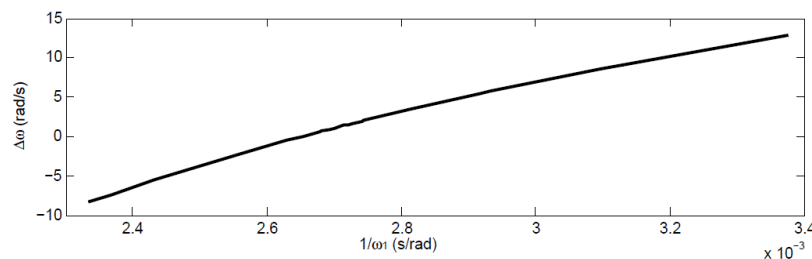


Figure 4: Variation of rotor speed error due to rotor current angular velocity inverse with 50% error in mutual inductance.

Among all the effects of parameter variations, the mutual inductance error has the most significant influence on the rotor speed estimation and rotor angular velocity.

For validation, simulation results are carried out to verify the effect of machine parameter variations in the computation algorithm. The results are presented in Section IV.

SIMULATION STUDIES

Figure 5 shows the rotor-side converter control scheme for the decoupled control of stator active and reactive power. The rotor currents are controlled in amplitude, frequency, and phase with a current-controlled pulse width modulation voltage source inverter on the rotor side by applying suitable rotor voltages. The stator-flux-oriented control is used for decoupling the active and reactive current control loops. The grid-side converter has to maintain a constant dc link voltage and regulates the grid-side reactive power using the conventional vector control approach. The parameters of the DFIG and control system are given in the Appendix. Simulations of the sensorless vector control system, shown in Figure 5, for a 1.5-MW DFIG are carried out using MATLAB/Simulink. In this study, a simulation for a complete wind generation system including a sensorless controlled DFIG-based wind turbine using the proposed algorithm is carried out. A wind speed model shown in Figure 6 is used as the input wind profile. The rated wind speed is assumed to be 13 m/s, and the optimal rotor speed of the DFIG at the rated condition is 1.2 p.u. For wind speeds higher than rated, the turbine energy capture is limited by applying pitch control.

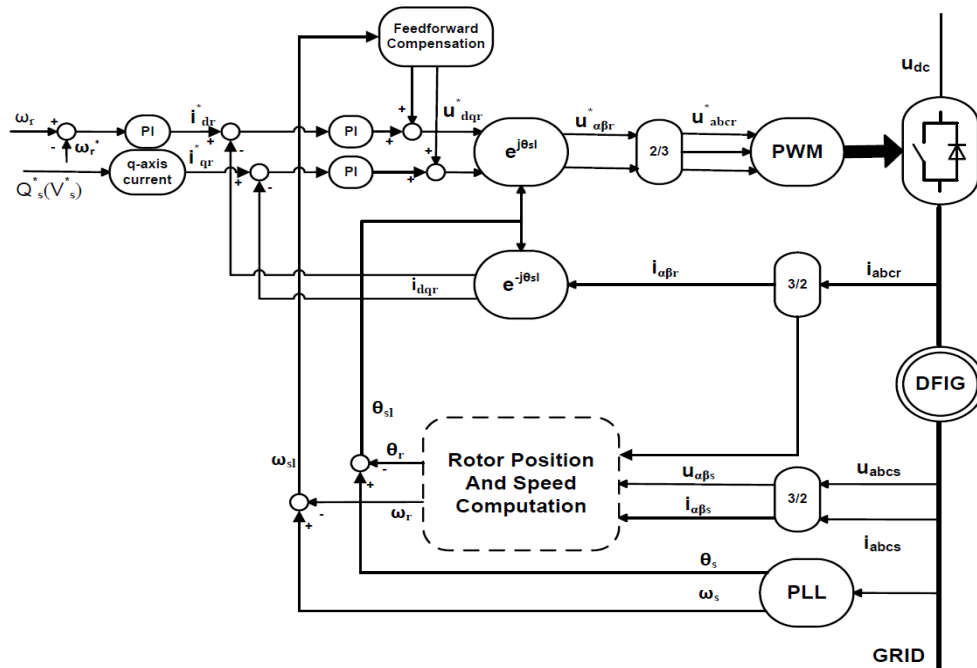


Figure 5: Sensor less vector control of DFIG.

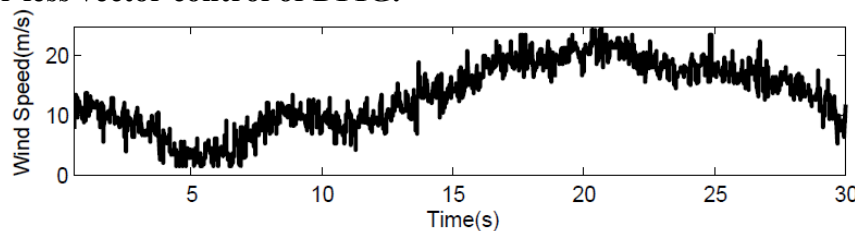


Figure 6: Wind speed model as input to wind turbine.

The DFIG is torque controlled in the simulation, and the torque current i_{qr} is proportional to the square of the estimated rotor speed, such that the maximum active power can be extracted from the wind and transferred to the grid. The active and reactive powers of the DFIG are shown in Figure 7. It can be clearly seen that rotor power P_r flows from the grid to the DFIG at sub synchronous speeds and in the opposite direction at super synchronous speeds. P_{grid} is the actual power delivered to the grid. The stator reactive power is regulated at around zero.

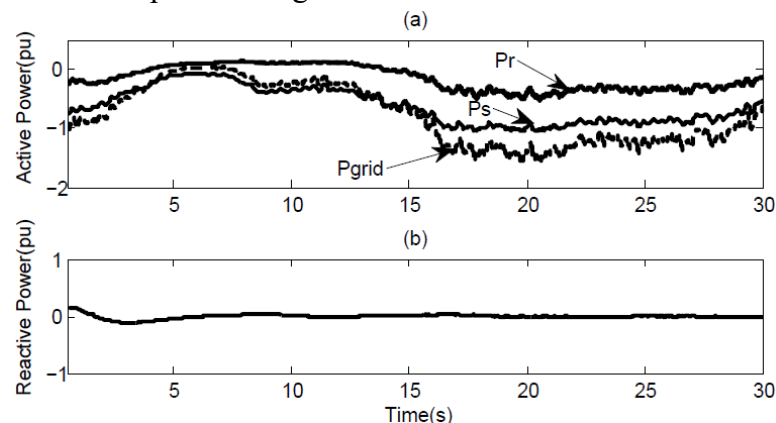


Figure 7: Generator active and reactive powers.

The DFIG rotor speed and estimation errors of the speed and position are shown in Figure 8. The estimated speed is very close to the actual speed during this fast transient process, with the speed error of less than 3% and the position error of less than 3°. The electromagnetic torque and various currents are plotted in Figure 9. It can be observed that T_{em} and i_{ds} are proportional to i_{dr} because of the stator flux orientation.

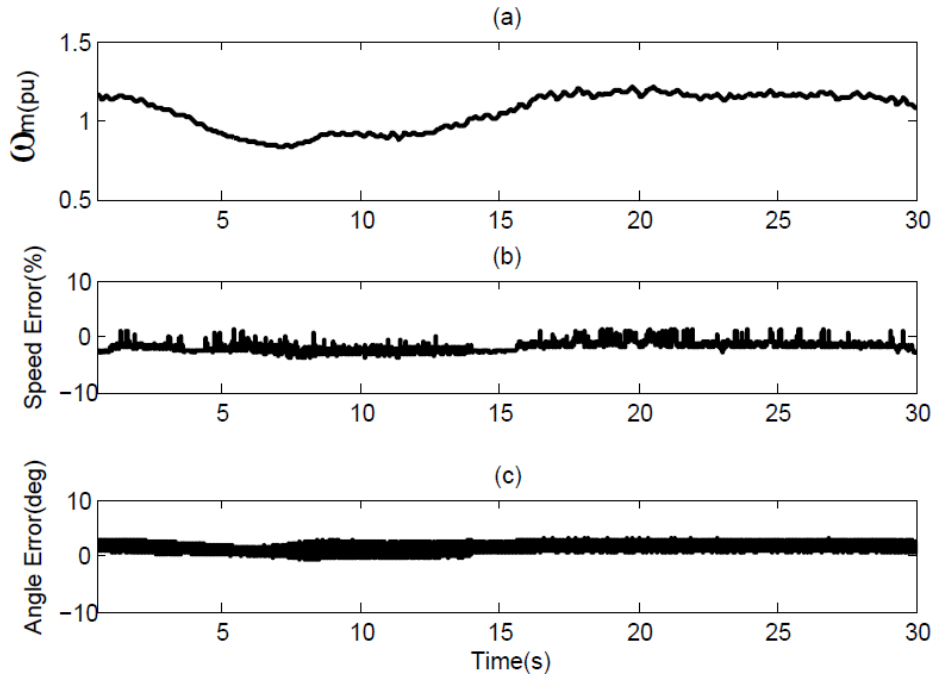


Figure 8: Actual and estimated rotor speeds and positions.

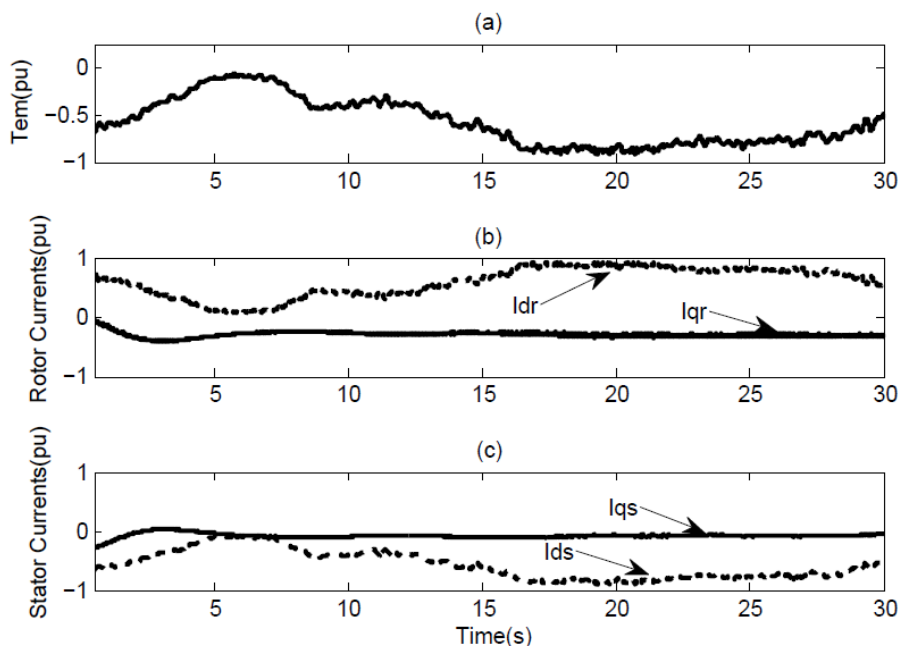


Figure 9: Electromagnetic torque and currents.

Finally, the effects of parameter variations on the sensorless controlled DFIG-based wind turbine using different estimation approaches are investigated. The wind speed is assumed to be 10 m/s initially and increases to 13 m/s at $t = 2$ s. Effects of various types of parameter variations, including the mismatch of stator resistance, stator leakage inductance, and mutual inductance, are investigated. When parameter mismatch occurs, only the situation where the actual parameter of the DFIG is larger than its nominal value used in the control system is examined because this happens more likely in reality. The parameter mismatch is assumed to occur at $t = 0$. The results are organized in Figure 10. It can be observed that the computational method is sensitive to the mutual inductance mismatch. The rotor electrical angle error is 10° when the actual mutual inductance is 50% larger than its nominal value. In the case of stator leakage inductance and rotor resistance mismatch, the estimated rotor angle has relatively the 3° error.

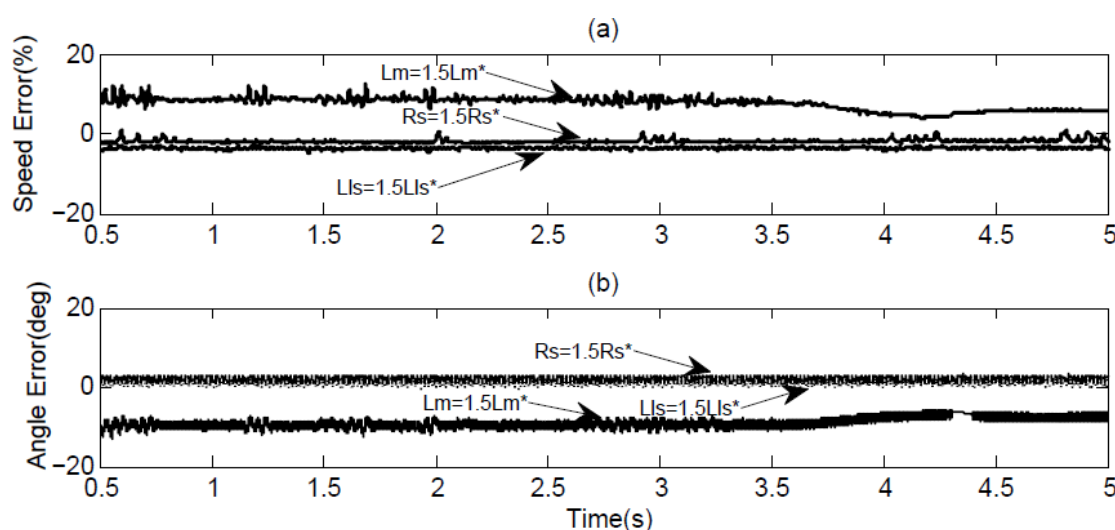


Figure 10: Parameter variation effects (a) Rotor mechanical speed error. (b) Rotor electrical angle error.

CONCLUSION

This paper presents a new, unique and straightforward method for the estimation of the rotor position and speed in sensorless vector control of DFIGs. The algorithm is a very implicit procedure and there is no need for computing the stator flux. Overall, this paper presents a potential technique for computing the rotor position which is simple and innovative. Effects of parameter variations on the steady state and dynamic performance have been investigated and the performance of the system is considerably independent of the system parameters. It depends weakly on the mutual inductance L_m parameter. Implementation on a real-time digital simulator is the subject of the ongoing research.

APPENDIX

DFIM data and parameters: Rated apparent power $S = 1.5/0.9$ MVA, rated power $P = 1.5$ MW, (stator Y/rotor Y) 575/1975 V, frequency $f = 60$ Hz, $R_s = 0.023$ p.u., $R_r = 0.016$ p.u., $L_m = 2.9$ p.u., $L_{ls} = 0.18$ p.u., $L_{lr} = 0.16$ p.u., inertia constant $H = 0.685$ s, and pole pairs $n_p = 3$.



REFERENCES

- Amuthan N., Subburaj P. and Mary P. M. (2013).** Direct model reference adaptive internal model controller for better voltage sag ride through in doubly fed induction generator wind farms. *Int. J. Electrical Power Energy Systems*. 47: 255-263.
- Chena C. H., Honga C.-M. and Chengb F.-S. (2012).** Intelligent speed sensorless maximum power point tracking control for wind generation system. *Int. J. Electrical Power Energy Systems*. 42(1): 399-407.
- Datta R. and Ranganathan V. T. (2001).** A simple position-sensorless algorithm for rotor-side field-oriented control of wound-rotor induction machine. *IEEE Transactions Industrial Electronics*. 48(4): 786-793.
- Dezza F. C., Foglia G., Iacchetti M. F. and Perini a. R. (2012).** An mras observer for sensorless dfim drives with direct estimation of the torque and flux rotor current components. *IEEE Transactions On Power Electronics*. 27(5): 2576 - 2584.
- Hu J., Nian H., Hu B., He Y. and Zhu Z. Q. (2010).** Direct active and reactive power regulation of dfig using sliding-mode control approach. *IEEE Transactions Energy Conversion*. 25(4): 1028 - 1039.
- Iacchetti M. F. (2010).** On line tuning of the stator inductance in a mras observer for sensorless dfim drives. *XIX International Con. Electrical Machines - ICEM 2010*. 1 - 6.
- Iacchetti M. F. (2011).** Adaptive tuning of the stator inductance in a rotor-current-based mras observer for sensorless doubly fed induction-machine drives. *IEEE Transactions Industrial Electronics*. 58(10): 4683 - 4692.
- Karthikeyan A., Nagamani C., Chaudhury A. B. R. and Ilango G. S. (2012).** Implicit position and speed estimation algorithm without the flux computation for the rotor side control of doubly fed induction motor drive. *IET Electric Power Applications*. 6(4): 243-252.
- Krzeminski Z., Popenda A., Melcer M. and Ladach P. (2001).** Sensorless control system of double fed induction machine with predictive current controller. *European Power Electronics Con.(EPE)*.
- Marques G. D., Pires V. F. A., Sousa S. e. and Sousa D. M. (2011).** A dfig sensorless rotor-position detector based on a hysteresis controller. *IEEE Transaction on Energy Conversion*. 26(1): 9-17.
- Marques G. D. and Sousa D. M. (2011).** Air-gap-power-vector-based sensorless method for dfig control without flux estimator. *IEEE Transactions Industrial Electronics*. 58(10): 4717-4726.
- Marques G. D. and Sousa D. M. (2012).** New sensorless rotor position estimator of a dfig based on torque calculations-stability study. *IEEE Transactions Energy Conversion*. 27(1): 196 - 203.
- Muller S., Deicke M. and Doncker R. W. D. (2002).** Doubly fed induction generator systems for wind turbines. *IEEE Industry Applications Magazine*. 8(3): 26-33.
- Ourici A. (2012).** Double flux orientation control for a doubly fed induction machine. *Int. J. Electrical Power Energy Systems*, 43(1): 617-620.
- Pena R., Cardenas R., Proboste J., Asher G. and Clare J. (2008).** Sensorless control of doubly-fed induction generators using a rotor-current-based mras observer. *IEEE Transactions Industrial Electronics*. 55(1): 330 - 339.
- Shehata E. G. and Salama G. M. (2013).** Direct power control of dfigs based wind energy generation systems under distorted grid voltage conditions. *Int. J. Electrical Power Energy Systems*. 53: 956-966.



Tapia G., Tapia A. and Ostolaza J. X. (2006). Two alternative modeling approaches for the evaluation of wind farm active and reactive power performances. *IEEE Transactions Energy Conversion*. 21(4): 909-920.

Teja A. V. R., Chakraborty C., Maiti S. and Hori Y. (2012). A new model reference adaptive controller for four quadrant vector controlled induction motor drives. *IEEE Transactions Industrial Electronics*. 59(10): 3757 - 3767.

Tremblay E., Atayde S. and Chandra A. (2011). Comparative study of control strategies for the doubly fed induction generator in wind energy conversion systems: A dsp-based implementation approach. *IEEE Transactions Sustainable Energy*. 2(3): 288 - 299.

Vas P. 1998. *Sensorless vector and direct torque control*, London, U.K.: Oxford Univ. Press.

Yang S. and Ajjarapu V. (2010). A speed-adaptive reduced-order observer for sensorless vector control of doubly fed induction generator-based variable-speed wind turbines. *IEEE Transactions On Energy Conversion*. 25(3): 891 - 900.

Zhang Y., Li Z., Wang T. and Hu J. (2011). Predictive direct torque and flux control of doubly fed induction generator with switching frequency reduction for wind energy applications. *Int. Con. Electrical Machines Systems (ICEMS)*, 1-6.

Zhi D. and Xu L. (2007). Direct power control of dfig with constant switching frequency and improved transient performance. *IEEE Transactions Energy Conversion*. 22(1): 110 - 118.